J Appl Electrochem (2010) 40:1069–1078
DOI 10.1007/s10800-009-0061-6

ORIGINAL PAPER

Electrokinetic phosphorus recovery from packed beds of sewage sludge ash: yield and energy demand

Georg Sturm · Harald Weigand · Clemens Marb · Wilfried Weiß · Bernd Huwe

Received: 18 September 2009 / Accepted: 21 December 2009 / Published online: 4 February 2010

Abstract The static lifetime of primary phosphate stocks is estimated as one century. Thus, the exploitation of secondary phosphorus sources becomes increasingly important. This study focussed on the feasibility of an electrokinetic phosphorus recovery from sewage sludge ash (P-content ~5 wt%). Packed bed experiments were conducted under varied electric conditions with and without acid pre-treatment and employing porous and ion exchange materials as electrode wells. Maximum values of phosphate concentration obtained in all experiments were around 2.5 g L^{-1}. Galvanostatic conditions were superior to potentiostatic conditions and acid pre-treatment is preferable over packed bed saturation with water. Ion-exchange membranes improved the product quality but increased the energy demand. Phosphorus recovery below 1% of the initial contents shows that the recovery setup must be improved in view of a marketable application.

G. Sturm (✉) · C. Marb
Bavarian Environment Agency, Josef-Vogl-Technology-Centre, Am Mittleren Moos 46, 86167 Augsburg, Germany
e-mail: georg.sturm@lfu.bayern.de

H. Weigand
Department of KMUB, Environmental Engineering, University of Applied Sciences Gießen-Friedberg, Wiesenstr. 14, 35390 Gießen, Germany

W. Weiß
Department of Protection of Labour and Environment, State Institute for Environment, Measurements and Nature Conservation Baden-Württemberg, Hertzstraße 173, 76187 Karlsruhe, Germany

B. Huwe
Soil Physics Group, University of Bayreuth, Universitätsstraße 30, 95440 Bayreuth, Germany

Keywords Phosphorus recovery · Sewage sludge ash · Electrokinetics

1 Introduction

Current population growth rates require an increased supply of staple foods. As a precondition, a sufficient nutrient level of agricultural soils needs to be maintained by application of soil fertilisers. One indispensable nutrient for plant growth is phosphate. Static lifetime of primary phosphate stocks (defined as economically minable deposits divided by actual annual consumption) is estimated as one century [1]. In addition, quality deterioration of the raw material has been observed by contamination with uranium and cadmium [2]. This has increased processing costs to meet the quality standards of mineral fertilizers [3].

In view of the above, the use of phosphate from secondary raw materials has turned into focus. One possible source of almost ubiquitous availability is municipal sewage sludge [4]. Its substitution potential for German primary phosphate imports has been estimated as 40% [5]. In many industrial countries the nutrient contents have been used in agriculture by direct application of sewage sludge to the soil. However, increasing awareness of sewage sludge contamination by persistent organic compounds [6] has caused doubt on the sustainability of this practice. In some countries the agricultural use has been banned [7] and the thermal treatment of sewage sludge is regarded as a better option.

During incineration, phosphorus (P) is enriched in the sewage sludge ash (SSA) yielding P-contents of up to 9% [7, 8]. In recent years efforts have been made to recover high quality phosphate from SSA [9]. This may be done by

(sequential) acid dissolution to release phosphate from low solubility phases [10]. Heavy metals co-eluted under acidic conditions can be removed by selective precipitation of phosphate minerals or ion exchange. An alternative is the metallurgical/thermochemical treatment of the ash. Thereby, a metal-depleted solid residue is produced with high contents of plant-available P [11, 12].

Although some of the technologies have already been implemented on a larger scale the maturity and cost-effectiveness has been questioned [7, 10, 13]. Another recovery technique could be the application of electrokinetics. These have been extensively studied in the context of desalination and crack closure of concrete, re-impregnation of wood, removal of heavy metals from contaminated materials (i.e. soil, fly ash, waste wood and mine waste), injection of nutrients in bioremediation and removal of organic contaminants, among others [14].

2 Electrokinetics in phosphorus recovery

Electrokinetic phenomena are induced in moist porous media by application of a direct current (DC) electric field which causes a transport of water, ions and charged particles towards the electrodes. Depending on the electric resistance of the porous media the energy inputs are partly converted into heat. This effect is referred to as Joule heating and its magnitude is proportional to the value of the electric current times voltage (≡electric power).

An electrokinetic setup consists of external hardware including a power source, electrodes and the connection between both. There, the current is transported by electrons (electron conduction) whereas in the porous medium the current flow is maintained by ions (ion conduction). For optimum conduction the electrodes are typically inserted in wells through which electrolytes are circulated. The transfer from electron conduction in the external hardware to ionic conduction in the medium happens by redox reactions at the electrode surfaces. These may involve reduction of metal cations, oxidation of chloride or, most importantly, water electrolysis (Eq. 1 and 2) [15].

$$\text{Anode: } H_2O \Rightarrow \frac{1}{2}O_2(g) + 2H^+ + 2e^- \quad (1)$$

$$\text{Cathode: } 2H_2O + 2e^- \Rightarrow H_2(g) + 2OH^- \quad (2)$$

In some cases it may be desirable to prevent the water electrolysis products (protons, hydroxide ions) from entering the medium, e.g. by use of ion-exchange membranes [16–18].

This study aims at the electrokinetic treatment of SSA as an alternative phosphate recovery method. Contrary to most heavy metals, phosphate in the pore water exists as anionic species unless the pH is strongly acidic. Thus, when a direct current is applied to water saturated SSA, phosphate, among other anions may selectively accumulate in the anolyte.

The pore water pH may influence the efficacy of an electrokinetic phosphate recovery from SSA in multiple ways. First, the dissolution of phosphate minerals is increased under acidic conditions due to the pH-dependent solubility of SSA-borne P-phases [10]. Second, the pH determines the affinity of dissolved phosphate towards variable charge surfaces, e.g. Al- and Fe(hydr)oxides [19]. Third, the transport velocity in an electric field is influenced by ionic charge and thereby dependent on the chemical speciation. For phosphate four speciation states, namely H_3PO_4, $H_2PO_4^-$, HPO_4^{2-} and PO_4^{3-} need to be considered. The corresponding acidity constants (pK_a, 298 K) are 2.12, 7.2, and 12 [20]. At pH below 2, phosphate dominantly exists as phosphoric acid and has no electric charge. Thus, it is unaffected by the electric field. Under alkaline conditions (pH > 7), the bi- and trivalent species prevail, which implies a double or triple amount of energy to move one phosphate ion.

A series of packed bed experiments were conducted under varied electric conditions, with and without acid pre-treatment of the ash. To separate the sewage sludge ash from the electrolytes both porous wells and ion exchange membrane wells were used. The feasibility of the method was evaluated by the purity of the product, the phosphate recovery efficiency and the energy demand.

3 Materials and methods

3.1 Sewage sludge ash

The sewage sludge ash was collected from a circulating fluidised bed incinerator for mechanically dewatered municipal sewage sludge. In compliance with the German Ordinance on Waste Incineration and Co-Incineration (17. BImSchV) incineration takes place at a temperature of 850 °C. The SSA is separated from the flue gas by an electrostatic filter and stored in an ash silo. From there a sample mass of 500 kg was taken, stored in polyethylene drums, and transported to the laboratory.

3.2 Experiment design

The electrokinetic phosphate recovery was studied in water-saturated packed beds (PB). Process efficiency was tested under constant voltage (potentiostatic) and constant current (galvanostatic) conditions. Whether or not phosphate recovery requires a pre-treatment of the SSA was assessed by saturating the PB with deionised water and mineral acids. In three experiments (I–III), porous wells

were used to separate the electrodes from the PB. Thereby, electrolysis products were allowed to spread in the PB. This may affect both the phosphate mobilisation (increased solubility at low pH), and the chemical composition of the anolyte (product purity). As an alternative well material, ion-selective membranes were tested in experiment IV. A preliminary check regarding energy consumption showed that electrode geometry (rod vs. plate) had a minor influence on the phosphate recovery. However, circulation of the electrolytes in tubular wells was deemed easier. Therefore, rod electrodes were used in all further tests.

3.3 Experimental setup and instrumentation

Experiments were conducted in boxes made of PMMA (polymethyl methacrylate, dimensions: 500 × 270 × 440 mm, l × w × h). On average, 17 kg SSA was filled into the boxes above a filter layer of silica sand (total PB volume: ca. 36 L). After the experiments the pore water of the SSA could be drained into the filter layer. The PBs were saturated from bottom to top to minimise air entrapment. To prevent corrosion by chlorine gas possibly evolved from anodic oxidation of chloride, the boxes were sealed with a lid and attached to the exhaust system. A liquid level-controlled irrigation system served to compensate water losses by evaporation.

The tubular porous polyethylene wells (inner diameter 60 mm) were purchased from Intus (Berlin, Germany). Cation and anion exchange wells (EDCORE®, Astom, Tokyo, Japan) were obtained from Alting (Strassbourg, France). Iridium oxide-coated titanium anodes and stainless steel cathodes were also provided by Alting. After placing the wells into the boxes the electrodes were inserted and connected to a DC power supply providing a maximum voltage and current of 200 V and 3 A (Statron, Fuerstenwalde, Germany).

Tygon® tubes (Saint-Gobain Performance Plastics Verneret, Charny, France) attached to peristaltic pumps (BVP-Standard, Ismatec, Wertheim-Mondfeld, Germany) were used to rinse the electrodes and circulate the anolyte and catholyte through separate, continuously stirred storage tanks. Electrode well volumes of 0.6 L and circulation rates of 14.4 L h^{-1} resulted in mean well water residence times of 2.5 min.

Instrumentation of the PBs (Fig. 1) included four platinum wires to monitor the potential drop, four thermocouples for temperature measurement (UMS, Munich, Germany), and three polyethylene suction cups with nylon membranes of 0.2 µm pore size (MacroRhizon SMS, Eijkelkamp, Giesbeek, The Netherlands). The latter were used to follow the pH, electric conductivity and dissolved phosphate in the PBs. Electric parameters and temperature were recorded every minute with a JUMO Logoscreen data acquisition system (JUMO, Fulda, Germany). To avoid overheating of the setup, a maximum operation temperature of 348 K was defined. Temperature readings exceeding this limit caused an automatic shutdown of the power supply.

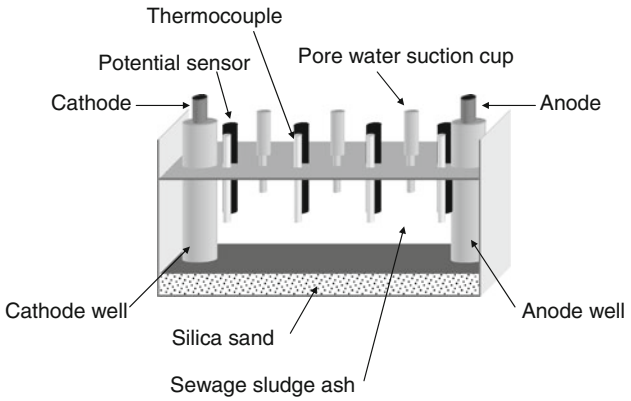

Fig. 1 Experimental setup and instrumentation for electrokinetic recovery of phosphorus from sewage sludge ash

3.4 Experimental conditions

The experimental conditions are summarised in Table 1. In experiment I–III porous polyethylene wells were employed, while cation and anion exchange wells were used in experiment IV. The dry mass of the packed beds and bulk density was approximately equivalent throughout. Experiment I was performed under potentiostatic conditions of 100 V. The experiments II–IV were carried out at a constant current (experiment II and III: 1 A, experiment IV: 0.3 A). A lower current was chosen in experiment IV to avoid exceedance of the limiting current density of the anion exchange membrane and concomitant energy losses caused by water splitting [22].

3.5 Sampling and analysis

The anolyte and catholyte were sampled daily. Using a syringe, 50 mL of electrolyte were extracted from the corresponding stirred storage tank. The volume was replaced with deionised water and the samples were membrane filtrated (Minisart® NML Syringe Filter, pore size: 0.45 µm, Sartorius Stedim Biotech GmbH, Goettingen, Germany). Pore water was collected daily by applying a pressure head of −25 kPa to the suction cups via a controlled vacuum system. Due to the configuration of the suction cups (see Sect. 3.3), filtration was not necessary. At the end of the experiments the packed beds were freely drained and an aliquot of the bulk pore water was sampled.

Table 1 Experiment parameters of electrokinetic phosphorus recovery experiments

Experiment	I	II	III	IV
Duration t_{max} (h)	184	261	189	236
Well material (–)	Porous polyethylene	Porous polyethylene	Porous polyethylene	Ion exchange membranes
Packed bed				
$Mass_{dry\ matter}$ (kg)	18.5	17.9	16.8	16.9
Bulk density (kg L^{-1})	0.93	0.90	0.84	0.85
Porosity n[a] (–)	0.65	0.66	0.69	0.68
Saturation solution				
Volume (L)	21.5	21.9	22.2	17.9
pH (–)	7.5	7.5	1.4	1.1
Electric conditions	Potentiostatic	Galvanostatic	Galvanostatic	Galvanostatic
Voltage (V)	100	Variable	Variable	Variable
Current (A)	Variable	1.0	1.0	0.3

[a] $n = 1 - (\rho_B/\rho_F)$ [21] with ρ_B bulk density and ρ_F substance density of SSA (2.68 g cm^{-3})

In all aqueous samples (electrolytes and pore water) the pH and electric conductivity were determined with a Sen Tix 81 pH-combination electrode (WTW, Weilheim, Germany) and a TetraCon 325 conductance probe (WTW), respectively. Ion-exchange-chromatography (Modular IC, Metrohm, Herisau, Switzerland) was employed to analyse the ortho-phosphate concentration in the samples. By crosschecks the presence of polyphosphate could be ruled out. Electrolytes and pore water were additionally analysed for Al, Ca, Cd, Cu, Cr, Fe, K, Mg, Ni, P, Pb, and Zn. Both Inductively coupled-plasma Mass-spectrometry (ICP-MS, Agilent 7500 cx, Agilent Technologies, Boeblingen, Germany) and Inductively coupled-plasma Optical-emission-spectrometry (ICP-OES, TJA IRIS, Thermo, Dreieich, Germany) were used. Compared to phosphate determination ICP analyses were carried out at a lower temporal resolution.

The solid phase composition of the SSA was analysed by X-ray fluorescence spectroscopy (XRF) in fivefold replication (Spectro XEPOS+, Spectro Analytical Instruments, Kleve, Germany). To characterise the mineralogy of the SSA, powder X-ray diffraction (XRD) was performed with a D5000 (Siemens, Madison WI, USA) including Rietveld refinement. The acid neutralisation capacity of the SSA was quantified in pH_{stat} experiments employing a titroprocessor (Titrando 836, Metrohm, Herisau, Switzerland). A target pH of 2.5 was held constant over 2 h. These deviations from the method suggested in the German Landfill Ordinance (DepV, annex 4, pH 4, 24 h equilibration) were adopted to account for the need of a fast P-mobilisation and for the fact that hardly any phosphate could be solubilised at pH 4. Substance density was analysed by pyknometry (AccuPyc 1330, Micromeritics, Moenchengladbach, Germany).

4 Results and discussion

4.1 Composition and physicochemical properties of sewage sludge ash

The fine grained SSA ($d_p < 500$ μm) has a water content of typically less than 0.15 wt% and behaves moderately alkaline (pH 9.5). The acid neutralisation capacity (ANC, pH 2.5, 2 h equilibration) and substance density are 3.66 mol H^+ kg^{-1} and 2.68 g cm^{-3}, respectively. The ANC of the solid phase is connotative of a high buffer capacity (alkalinity). The latter results from the consumption of protons during the dissolution of mineral constituents and from the protonation of variable charge surfaces. Since the phosphate minerals themselves are largely insoluble unless the pH is highly acidic, a large amount of acid is necessary for a sufficient phosphorus mobilisation. Our data corroborate findings by Levlin et al. [10] who reported hydrochloric acid additions equivalent of 5 mol H^+ kg^{-1} to release around 80% of the P contents of SSA.

XRF results showed that silicium, calcium, iron, phosphorus, and aluminium are the major constituents of the solid phase, see Table 2.

This reflects (i) the waste water composition, (ii) the cleaning process, and (iii) the sewage sludge incineration. Iron and aluminium are partly introduced as precipitation agents to remove phosphate from the waste water stream. Sewage sludge containing up to 5.6 wt% silicium (dry matter) [23] and silica sand used for operating the circulating fluidised bed cause the high silicium content. The high phosphorus level mirrors the P-load of the waste water and its concentration in the SSA by water purification and incineration. The P-content of 48 g kg^{-1} agrees with published values [4, 7, 8].

Table 2 XRF-analyses of sewage sludge ash for selected elements

Element	Content	Element	Content	Element	Content
Al	31,420	Fe	53,180	Si	92,040
As	8.4	K	12,280	Sn	90.6
Ba	834	Mg	12,480	Sr	383.8
Br	30.8	Mn	595.6	Ti	3,886
Ca	89,980	Mo	21.8	Tl	<5
Cd	<5	Ni	76	U	18
Cl	<500	P	48,000	V	62
Co	<50	Pb	105.6	Y	34.6
Cr	107.2	Rb	65.6	Zn	2,244
Cu	703	S	8,290	Zr	143.8

Values in mg kg^{-1}

According to powder XRD analyses amorphous matter accounts for approximately 40 wt% of the SSA. Whitlockite, Enstatite, Brushite, and Hilgenstockite were identified as important P-phases. The corresponding contents (20.4, 3.9, 1.4, and 0.6 wt%, respectively) explain roughly 90% of the total P content. The remainder may be related to the amorphous fraction or exists as surface complexes (e.g. sorbed at iron oxides [19]).

4.2 Electrokinetic recovery experiments

4.2.1 Development of pH and electric conductivity

All recovery experiments were accompanied by a pronounced acidification of the anolyte and alkalinisation of the catholyte. Typically, within 24 h the corresponding pH reached values of around 1 and 12, pointing to intensive water electrolysis (cf. Eq. 1, 2). The final-pH established in the PBs varied among the experiments (Fig. 2). In experiment I and II (porous wells) the PB was saturated with deionised water (EC < 0.055 µS cm^{-1}, Seralpur Delta, USF Seral, Ransbach-Baumbach, Germany). Under these conditions and neglecting water electrolysis the pH is expected to correspond to the "native" pH of the SSA of 9.5 (DIN EN 38 404-5). This value was qualitatively met in pore water samples collected in the centre of the PB (pH_{centre}) previous and after the experiment. The corresponding values of the cathodic ($pH_{cathode}$) and anodic (pH_{anode}) regions of the PB after the experiment were 11.5 and 5.8, respectively. This indicates that water electrolysis caused a propagation of acid and base fronts through the packed bed. In experiment III (porous wells) the PB was saturated with an acidic solution (0.48 M, HNO_3) resulting in an initial pH of 3.5 (PB). At the end of the experiment, pH values were around 7.8 ($pH_{cathode}$), 6.1 (pH_{centre}), and 6.5 (pH_{anode}). The pH increase was most pronounced next to the cathode, since alkalinisation by water electrolysis

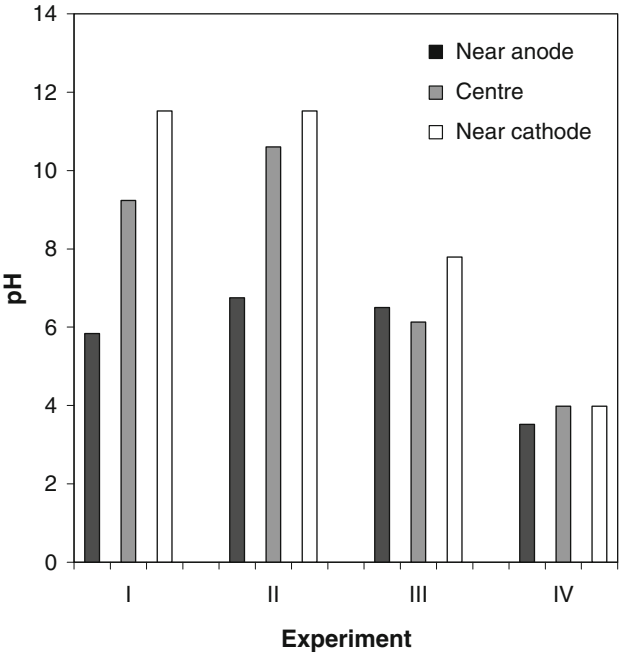

Fig. 2 pH value of pore water samples collected at the end of the experiments

and buffer reactions acted synergistically. Overall, the pH reflects the combined effects of buffer kinetics and the propagation of acid and base fronts.

In experiment IV membrane wells were combined with a more acidic saturation solution (0.6 M, H_2SO_4) resulting in an initial pH of 1.3 in the PB. Alike experiment III the final pH was markedly lower with values of 4 ($pH_{cathode}$, pH_{centre}) and 3.5 (pH_{anode}). Since the cation exchange membrane largely excluded water electrolysis products from the PB, the course of the pH in the centre and cathode sections of the PB primarily reflects the acid buffering by the SSA. This is supported by the congruence of the corresponding pore water pH-values against time (Fig. 3). Contrasting the centre and cathode sections, the pH of pore water samples collected close to the anode reached roughly constant values by day 5 of the experiment. This may point to partial failure of proton exclusion by the anion exchange membrane [24].

Pore water electric conductivities (EC) observed at the end of the experiments are summarised in Fig. 4. Neglecting both, electrolysis and buffer reactions within the PBs, ion accumulation in the wells should cause a gradual decline of pore water EC.

In experiment I and II the saturation with deionised water yielded initial EC values between 3.4 and 4 mS cm^{-1}. Final values of $EC_{cathode}$ and EC_{centre} were substantially lower, while the EC_{anode} showed a minor change.

In experiment III the acidic saturation solution gave rise to highly elevated EC values around 36 mS cm^{-1}. This

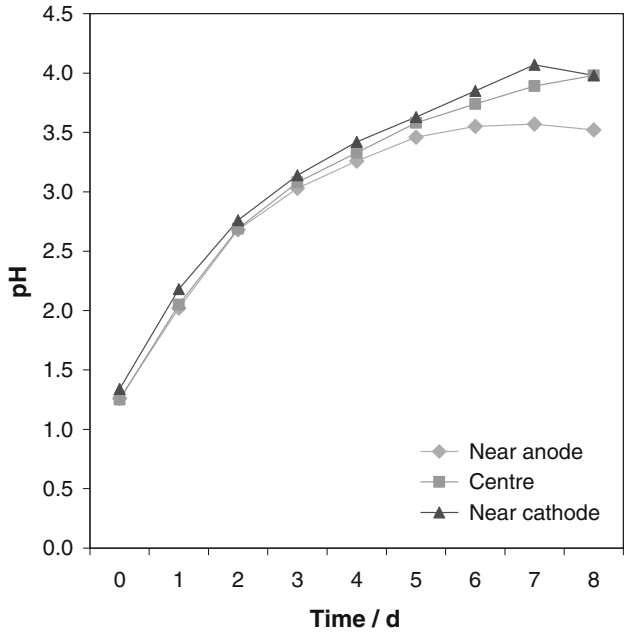

Fig. 3 Pore water pH development over time in experiment IV

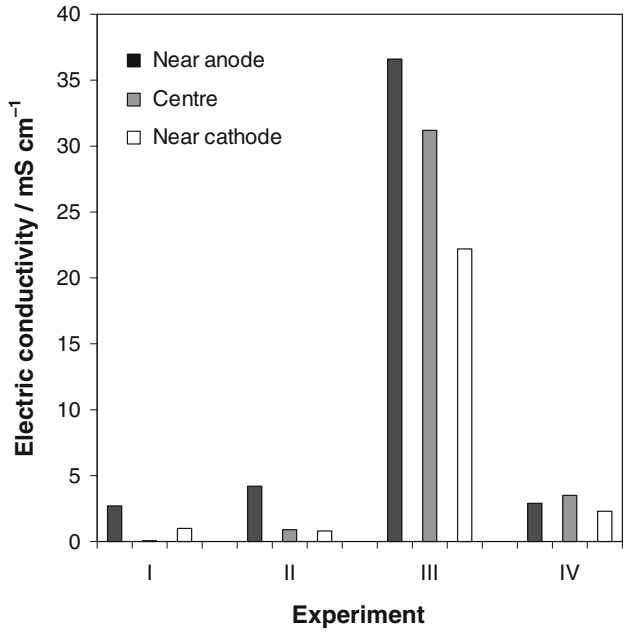

Fig. 4 Electric conductivity of pore water samples collected at the end of the experiments

reflects the enhanced dissolution of SSA constituents and the ionic strength of the saturation solution itself. A high conductivity was maintained in the anodic region while EC_{centre} and $EC_{cathode}$ declined to final values of 32 and 22 mS cm^{-1}, respectively.

High initial EC values caused by the acid treatment were also observed in experiment IV. Final values between 4 and 3 mS cm^{-1} were in the range of the initial values of experiment I and II.

The results substantiate a strong linkage between the pore water pH and the electric conductivity. Acid dissolution of SSA constituents introduces large amounts of charged species into the pore water. Buffer reactions cause a pH increase and thereby reduce the solubility of mineral components with a concomitant drop of the EC. When the acid front propagation is not impeded (porous wells), protons generated by water electrolysis counteract the buffer reactions and contribute to an elevated electric conductivity at the anode side. This explains the relative differences between $EC_{cathode}$ and EC_{anode} in experiments I to III. Conversely, when ion exchange membranes hamper the compensation of buffer reactions, the discrepancies between $EC_{cathode}$, EC_{centre} and EC_{anode} diminish.

4.2.2 Packed bed electric resistance and temperature

The PB electric resistance was calculated as the ratio of the potential drop between the Pt-probes installed in vicinity to the electrodes and the electric current. The development of resistance over time is shown in Fig. 5 (left). The horizontal axis represents a "dimensionless time" with t_{max} according to Table 1.

The temporal average of electric resistances follows the order: experiment I > experiment II > experiment IV $\gg$ experiment III. Except for the latter, the characteristics exhibit local minima shortly after experiment start. Higher resistances at the start of the experiments are due to the initially low electric conductivity of the saturation solution in experiment I and II (deionised water) and the membrane resistance which has to be overcome in experiment IV. The lack of a local minimum in experiment III may have resulted from the use of an acidic saturation solution in combination with porous wells. In all experiments the resistance increased over time. This reflects the evolution of pore water conductivities. Consequently, in experiment III the lowest PB resistance was observed.

Figure 5 (right) summarises the mean PB temperatures obtained from the four thermocouples. The ranking of the temporal average of temperatures agrees with the PB resistances. Temperature discontinuities in experiment I are due to shut downs of the power supply induced by PB temperatures exceeding 348 K (see Sect. 3.3). Typically, these were observed in vicinity of the cathode.

Experiment IV shows a local temperature minimum shortly after current application. In experiment III the highest temperature was observed at the beginning and then the PB slowly approached ambient conditions. This behaviour is indicative of exothermal reactions during saturation of the packed beds with acidic solutions.

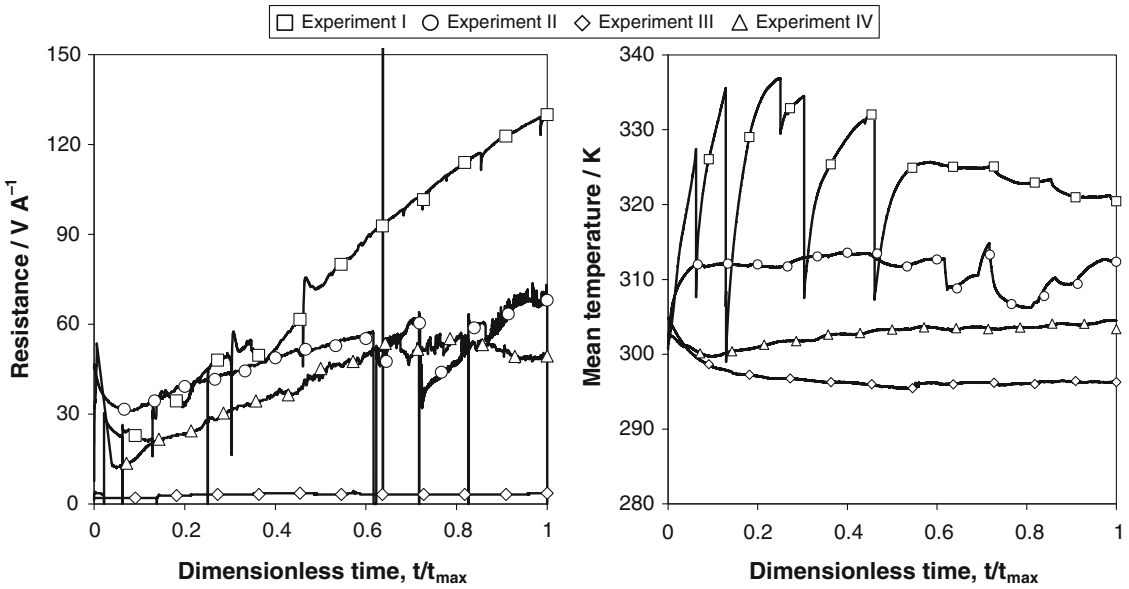

Fig. 5 Electric resistance of (*left*) and mean temperature (*right*) in the packed bed; t_{max} see Table 1

In experiment I maximum values of PB temperature coincided with lowest electric resistances. Potentiostatic conditions and a low PB resistance (high electric conductivity) resulted in a high electric current. Therefore, a high amount of energy is transferred into the PB promoting Joule heating. Conversely, galvanostatic conditions (experiment II to IV) lead to a more moderate potential drop (cf. Fig. 6). The vertical peaks in the course of experiment I result from breaks due to high temperatures (see Sect. 3.3). Since Joule heating is proportional to current times voltage, PB temperature stabilised at lower values in the following experiments.

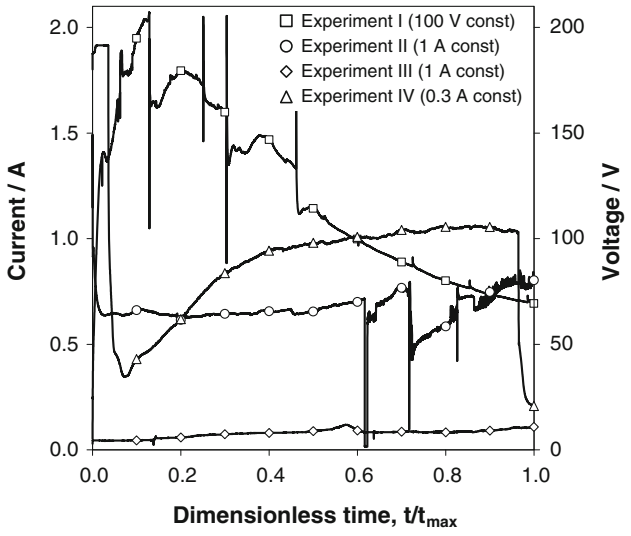

Fig. 6 Electric current and voltage progression during the experiments, Exp. I: var. current, Exp II–IV: var. voltage; t_{max} see Table 1

4.2.3 *Phosphate accumulation and phosphorus recovery efficiency*

To follow the accumulation of phosphate in the electrolytes, daily samples were collected. In all experiments, catholyte concentrations were negligible. In turn, high phosphate concentrations were observed in the anolyte. Figure 7 (left) illustrates the course of anodic phosphate accumulation in experiment II and IV against dimensionless time.

Experiment II was characterised by a fast increase of phosphate concentrations. After a maximum of 2.5 g L^{-1}, the level decreased following a parabolic characteristic. A similar behaviour and level was observed in experiment I.

Anodic precipitation of phosphates can be ruled out as a cause for the observed decrease in phosphate levels since the anolyte remained clear throughout. More likely, concentrations were influenced by the pH-dependent speciation of phosphate. At the low anolyte pH ($pH < 1.2$) undissociated and uncharged phosphoric acid is the dominant species. Hence, it is not attracted by the anode and may diffuse back through the porous well into the PB. Thus, the positive effect of anodic acidification at the beginning of the experiment (enhanced release of phosphate from solid phases) starts to work against phosphate accumulation.

Asides phosphate, the anolyte also exhibited high metal concentrations (Al: 1.1 g L^{-1}, Ca: 2 g L^{-1}, Cu: 5.9 mg L^{-1}, Fe: 0.4 g L^{-1}, K: 0.1 g L^{-1}, Ni: 1.2 mg L^{-1}, and Zn: 6.5 mg L^{-1}). Assuming a positive charge, these constituents would be expected to migrate towards the cathode. However, the catholyte did not substantiate this

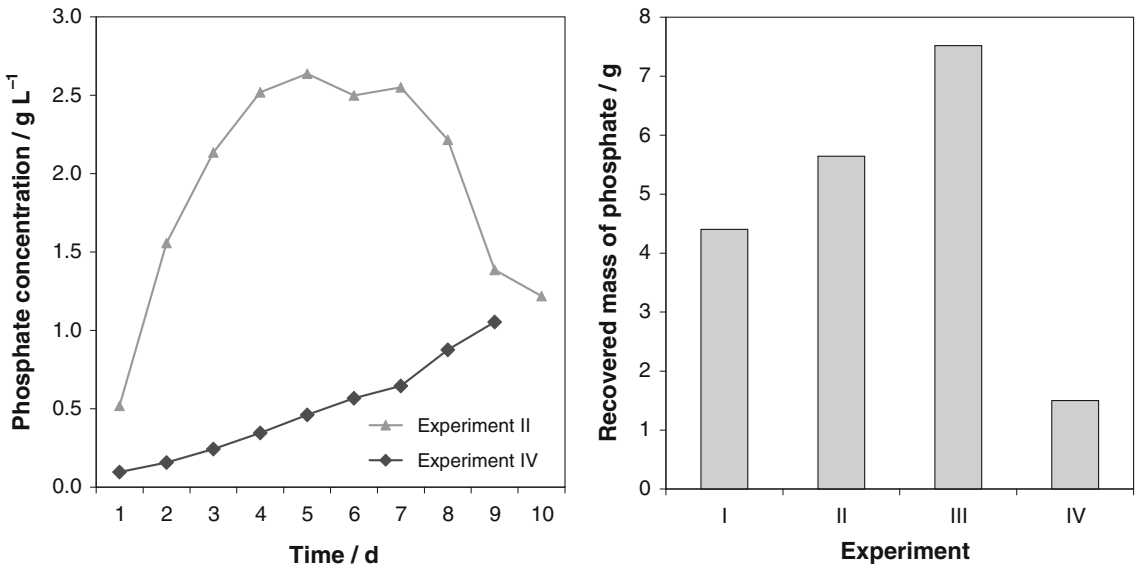

Fig. 7 Anodic phosphate accumulation (*left*), maximum absolute mass of phosphate in anode wells and pore-water (*right*)

hypothesis. Except for K and Ca all concentrations were lower than in the anolyte. This may indicate predominance of negatively charged metal complexes, which is, however, unlikely under low pH conditions. Alternatively, metals solubilised by the propagation of the acid front may have been passively introduced into the anolyte (e.g. by hydraulic gradients caused by circulation of well water).

The course of phosphate concentrations in the anolyte of experiment IV exhibited a different characteristic. The increase was almost linear over time. Yet, phosphate levels remained below the maximum observed in the tests carried out with porous wells (c_{max}: 1.0 g L^{-1}). The anion-exchange membrane impeded the evolution of an acid front. Thus, the pore water pH increased and phosphate mobilisation was hampered. Contrasting the findings of experiment I to III, the anolyte had noticeable lower contents of metals (Al: 14 mg L^{-1}, Ca: 30 mg L^{-1}, Cu: 0.2 mg L^{-1}, Fe: 3.5 mg L^{-1}, K: 4.7 mg L^{-1}, Ni: <50 µg L^{-1}, and Zn: 0.7 mg L^{-1}) indicating successful cation exclusion.

In experiment I–III precipitation products were recovered from the catholytes and dried. The fine grained white powder (up to 100 g) was analysed by XRF. Results showed large amounts of Al (2%), Ca (13%), Fe (1%), Mg (2%), and P (5%). This suggests that Ca-metal-phosphates (molar ratio: Ca:P:Mg:Al:Fe = 14:7:4:3:1) precipitated under alkaline conditions. Mineralogical analyses indicated that the product consisted of amorphous matter, only.

The total P recovery from the PBs is shown in Fig. 7 (right). In experiment II and III high phosphate concentrations were detected in pore water samples taken at the end of the experiments. The corresponding mass of P was included in the calculated P recovery. As discussed above, in experiment II the anolyte phosphate concentration decreased by day 7 (Fig. 7, left) probably due to back diffusion into the packed bed. To assess a possible overestimation of P recovery in this particular case, the difference between maximum and final mass of P in the anolyte was balanced against the mass of P in the pore water. Results indicated that potential overestimation of P recovery was less than 5%.

The amount of P recovered increased in the order: experiment IV < experiment I < experiment II < experiment III. Thus, galvanostatic conditions seem more favourable than potentiostatic conditions and acid pre-treatment enhances P recovery over saturation with deionised water. With respect to well materials the use of ion-exchange membranes yields a higher purity of the anolyte at the expense of lower P accumulation.

In experiment I–III the recovered P mass in the liquid phase (anolyte and pore water) amounted to a maximum of 7.5 g (experiment III). The lower yield of experiment IV (1.5 g) reflects the combined effects of membrane resistance and reduced P availability due to pH buffering by SSA.

The initial phosphorus content of the SSA used in the experiments was between 806 g and 888 g (see Table 3). Dividing the P-yield by initial contents resulted in a low recovery efficiency of less than 1% for all experiments.

4.2.4 Energy demand

The experimental conditions substantially influenced the energy demand of the electrokinetic phosphate recovery

Table 3 Phosphorus mass balance and recovery efficiency of the four experiments

Experiment	I	II	III	IV
Sewage sludge ash (initial content)				
Phosphorus mass (g)	888.0	859.2	806.4	811.2
Liquid phase content (recovery)				
Phosphorus mass (g)	4.4	5.6	7.5	1.5
Recovery efficiency (%)	0.5	0.7	0.9	0.2

Table 4 Electric energy data of the four experiments

Experiment	I	II	III	IV
Electric energy input (MJ)	78.5	62.4	5.4	22.0
Experiment duration (h)	184	261	189	236
Average electric power (kJ h^{-1})	426.6	239.1	28.6	93.2

(see Table 4). The average electric energy consumption follows the order: experiment I > experiment II > experiment IV > experiment III. Thus, the acid pre-treatment lowers the energy demand significantly compared to saturation with deionised water. Conversely, ion exchange membranes increase the energy consumption over porous well materials.

To gain insight into the economic feasibility of the electrokinetic P recovery approach, the energy data were related to the P yields. The energy input and time to reach local P-concentration maxima differed significantly in experiment I to IV. Results of the energy balance are shown in Table 5.

Taking the results of experiment I (potentiostatic conditions, saturation with deionised water and porous electrolyte wells) as a baseline, the galvanostatic conditions of experiment II cut the P-specific energy demand by 60%, approximately. Regarding the differences in PB temperature (see Sect. 4.2.2), lower Joule heating under galvanostatic conditions seems to be the primary cause of the efficiency increase.

The acid pre-treatment in experiment III shows a further reduction of energy expenses. A total of 0.2 MJ per g P is equivalent to energy savings of 98% compared to experiment I. This is consistent with a further reduction of Joule heating by the increased pore water conductivity. Also, the time to reach maximum P concentrations was reduced by 40%. This indicates that acid dissolution of P-phases promoted the availability of phosphate and rendered the process more efficient. The time to reach the maximum P concentration took approximately 2.5 days in experiment III. For the treatment of a higher mass of SSA (several tons per day) this time frame is not applicable.

In experiment IV (ion exchange membrane wells) the maximum P-specific energy input was observed. With 14.7 MJ $(g\ P)^{-1}$ the energy demand exceeded that of experiment I by 10%. This indicates that minimised anolyte contamination by heavy metals was counterbalanced by buffer reactions in the absence of the acid front. Recessive phosphate concentrations in pore water may have limited P accumulation in the anolyte in addition to the transport resistance of the ion-exchange membrane.

5 Conclusions and prospects

The experimental results show that electrokinetics in principle are a workable approach for P recovery from sewage sludge ash. Phosphate accumulation in the anolyte leads to concentrations in the range of g L^{-1}. However, process energetics are strongly dependent on the electric power input and the ash pre-treatment. With respect to energy losses galvanostatic conditions are superior to a constant voltage approach due to lower Joule heating. Acid pre-treatment enhances the P recovery over saturation with deionised water. Increased phosphate availability and electric conductivity result in a faster P transfer into the anolyte and a further reduction of Joule heating.

Porous electrode wells allow the evolution of acid and base fronts into the packed bed. This maintains a low pH in the anodic region and is beneficial for P availability on the local scale. However, metals are not excluded from the anolyte and contamination of the product may entail further purification steps. Conversely, the use of ion-exchange membranes yields a higher product purity at the expense of a lower recovery rate and higher energy input. Irrespective of the experimental conditions P recovery was below 1% of the initial contents. Hence, in spite of high anolyte concentrations the treatment seems economically unfeasible.

Table 5 Electric energy demand based on phosphorus recovery data

Experiment	I	II	III	IV
Duration[a] (h)	112	117	66	216
Electric energy consumption[a] (MJ)	58.8	27.5	1.4	22.0
Specific energy demand per gram phosphorus[a] (MJ g^{-1})	13.4	4.7	0.2	14.7

[a] Until maximum phosphate concentration was achieved

Therefore, further steps have to be taken to improve P recovery and the time frame of the treatment.

While an acid pre-treatment and the use of ion-exchange membranes are deemed necessary to enhance P availability and avoid anolyte contamination, the packed bed approach pursued in this study is too time consuming. Therefore, future optimisation of the process will focus on the electrokinetic treatment of SSA suspensions in continuously stirred tank reactors.

Acknowledgements We are indebted to Mr Georg Hiller for providing the sewage sludge ash from the municipal sewage sludge incineration plant Steinhaeule, Neu-Ulm, Germany. We also thank the members of the Analytical Department of the Bavarian Environment Agency for element analyses. Our special thanks go to the State Institute for Environment, Measurements and Nature Conservation Baden-Württemberg for funding this project.

References

1. Steen I (1998) Phosphorus Potassium 217:25–31
2. Guzmán RET, Ríos SM, García JLI, Regil EO (1995) J Radioanal Nucl Chem 189:301–306
3. Bunus FT (1994) In: Hodge CA, Popovici NN (eds) Pollution control in fertilizer production. Marcel Dekker, New York, pp 237–252
4. Herbst H, Montag D, Gethke K, Pinnekamp J (2007) KA Abwasser Abfall 54:1013–1024
5. Cornel P, Schaum C (2003) In: Rückgewinnung von Phosphor in der Landwirtschaft und aus Abwasser und Abfall. Symposium Proceedings, 6–7 February 2003, Berlin, organised by The Federal Environment Agency and the Institute of Environmental Engineering, RWTH Aachen University, Aachen
6. Harrison EZ, Oakes SR, Hysell M, Hay A (2006) Sci Total Environ 367:481–497
7. Franz M (2008) Waste Manag J 28:1809–1818
8. Adam C, Kley G, Simon F-G (2007) Mater Trans 48:3056–3061
9. Morse GK, Brett SW, Guy JA, Lester JN (1998) Sci Total Environ 212:69–81
10. Levlin E (2007) Phosphorus recovery with acid and base from inorganic sewage sludge residues. Water Pract Technol. doi: 10.2166/wpt.2007.018
11. Mattenberger H, Fraissler G, Brunner T, Herk P, Hermann L, Obernberger I (2008) Waste Manag J 28:2709–2722
12. Adam C, Peplinski B, Michaelis M, Kley G, Simon F-G (2009) Waste Manag J 29:1122–1128
13. Levlin E, Löwén M, Stark K, Hultman B (2002) Water Sci Technol 46:435–440
14. Ottosen LM, Christensen IV, Rörig-Dalgard I, Jensen PE, Hansen HK (2008) J Environ Sci Health A 43:795–809
15. Rajeshwar K, Ibanez J (1997) Environmental electrochemistry. Academic Press, London, pp 57–124
16. Hansen HK, Ottosen LM, Laursen S, Villumsen A (1997) Sep Sci Technol 32:2425–2444
17. Ribeiro AB, Mexia JT (1997) J Hazard Mater 56:257–271
18. Desharnais BM, Lewis BAG (2002) Soil Sci Soc Am J 66:1518–1525
19. Sims JT, Pierzynski GM (2005) In: Tabatabai MA, Sparks DL (eds) Chemical processes in soils. Book series 8. Soil Science Society of America, Madison, WI, pp 151–192
20. Cotton FA, Wilkinson G, Murillo CA, Bochmann M (1999) Advanced inorganic chemistry, 6th edn. Wiley, New York
21. Scheffer F, Schachtschabel P, Blume H-P, Brümmer GW, Schwertmann U, Horn R, Kögel-Knaber I, Stahr K, Auerswald K, Beyer L, Hartmann A, Litz N, Scheinost A, Stanjek H, Welp G, Wilke B-M (2002) Lehrbuch der Bodenkunde, 15th edn. Spektrum Akademischer Verlag, Heidelberg, p 163
22. Ottosen LM, Hansen HK, Hansen CB (2000) J Appl Electrochem 30:1199–1207
23. Thomé-Kozmiensky KJ (1998) Klärschlammentsorgung. TK Verlag Karl Thomé-Kozmiensky, Neuruppin, pp 114–116
24. Melin T, Rautenbach R (2007) Membranverfahren. Springer, Berlin, p 372